



Secretion of Recombinant Interleukin-22 by Engineered *Lactobacillus reuteri* Reduces Fatty Liver Disease in a Mouse Model of Diet-Induced Obesity

Jee-Hwan Oh,^a Kathryn L. Schueler,^b Donnie S. Stapleton,^b Laura M. Alexander,^a Chi-Liang Eric Yen,^c Mark P. Keller,^b Alan D. Attie,^b Jan-Peter van Pijkeren^a

^aDepartment of Food Science, University of Wisconsin—Madison, Madison, Wisconsin, USA

^bDepartment of Biochemistry, University of Wisconsin—Madison, Madison, Wisconsin, USA

^cDepartment of Nutritional Sciences, University of Wisconsin—Madison, Madison, Wisconsin, USA

ABSTRACT The incidence of metabolic syndrome continues to rise globally. In mice, intravenous administration of interleukin-22 (IL-22) ameliorates various disease phenotypes associated with diet-induced metabolic syndrome. In patients, oral treatment is favored over intravenous treatment, but methodologies to deliver IL-22 via the oral route are nonexistent. The goal of this study was to assess to what extent engineered *Lactobacillus reuteri* secreting IL-22 could ameliorate nonalcoholic fatty liver disease. We used a mouse model of diet-induced obesity and assessed various markers of metabolic syndrome following treatment with *L. reuteri* and a recombinant derivative. Mice that received an 8-week treatment of wild-type probiotic gained less weight and had a smaller fat pad than the control group, but these phenotypes were not further enhanced by recombinant *L. reuteri*. However, *L. reuteri* secreting IL-22 significantly reduced liver weight and triglycerides at levels that exceeded those of the probiotic wild-type treatment group. Our findings are interesting in light of the observed phenotypes associated with reduced nonalcoholic liver disease, in humans the most prevalent chronic liver disease, following treatment of a next-generation probiotic that is administered orally. Once biological and environmental containment strategies are in place, therapeutic applications of recombinant *Lactobacillus reuteri* are on the horizon.

IMPORTANCE In humans, nonalcoholic fatty liver disease (NAFLD) is the most prevalent liver disease due to the increased prevalence of obesity. While treatment of NAFLD is often geared toward lifestyle changes, such as diet and exercise, the use of dietary supplements such as probiotics is underinvestigated. Here, we report that probiotic *Lactobacillus reuteri* reduces fatty liver in a mouse model of diet-induced obesity. This phenotype was further enhanced upon delivery of recombinant interleukin-22 by engineered *Lactobacillus reuteri*. These observations pave the road to a better understanding of probiotic mechanisms driving the reduction of diet-induced steatosis and to development of next-generation probiotics for use in the clinic. Ultimately, these studies may lead to rational selection of (engineered) probiotics to ameliorate fatty liver disease.

KEYWORDS diet-induced metabolic syndrome, fatty liver disease, IL-22, *Lactobacillus reuteri*, probiotic, engineered probiotic, interleukin-22, nonalcoholic fatty liver disease, steatosis

The global epidemic of metabolic syndrome is a pressing health concern. Individuals diagnosed with metabolic syndrome are more susceptible to cardiovascular disease, type 2 diabetes, fatty liver, and some cancers, including breast, pancreatic,

Citation Oh J-H, Schueler KL, Stapleton DS, Alexander LM, Yen C-LE, Keller MP, Attie AD, van Pijkeren J-P. 2020. Secretion of recombinant interleukin-22 by engineered *Lactobacillus reuteri* reduces fatty liver disease in a mouse model of diet-induced obesity. *mSphere* 5:e00183-20. <https://doi.org/10.1128/mSphere.00183-20>.

Editor Maria L. Marco, University of California, Davis

Copyright © 2020 Oh et al. This is an open-access article distributed under the terms of the [Creative Commons Attribution 4.0 International license](https://creativecommons.org/licenses/by/4.0/).

Address correspondence to Jan-Peter van Pijkeren, vanpijkeren@wisc.edu.

Received 24 February 2020

Accepted 8 June 2020

Published 24 June 2020

colorectal, and prostate cancers (1). Key circulatory diagnostic markers of metabolic syndrome are hyperglycemia, high-density lipoprotein, and triglyceride (TG) levels, and one of the key risk factors of metabolic syndrome is obesity (body mass index [BMI] of ≥ 30 kg/m²) (1). In obese individuals, the liver is a key organ presenting abnormalities in glucose and lipid metabolism, which are associated with increased incidence of nonalcoholic fatty liver disease. As of today, behavioral changes are considered the main driver to revert metabolic syndrome, but medical intervention strategies are considered the first line of treatment (2). In both nonalcoholic and alcoholic liver disease models, interleukin-20 (IL-20) family cytokines reduce liver injury and inflammation (3). For example, interleukin-22 (IL-22), a member of the IL-20 subfamily, controls lipid metabolism in the liver via activation of the STAT3 signaling pathway and, consequently, reduces fatty liver disease (4). Therefore, IL-22 has great potential to serve as a therapeutic protein to reduce alcohol- and non-alcohol-induced fatty liver diseases (5).

Currently, eukaryotic and prokaryotic cells are exploited as factories to produce therapeutic peptides and proteins (TPPs). Due to instability and large complex structure, most TPPs are administered parenterally by intramuscular, intravenous, or subcutaneous injection. But there are disadvantages of injection, which leads to cannula-related infections and adverse reactions such as pain, discomfort, and skin necrosis (6). Therefore, nonparenteral routes such as oral, nasal, transdermal, and rectal administration have been tested to deliver TPPs. Among these alternatives, oral administration is the most favored route in patients (7).

Since the 1990s, live bacteria have been developed as factories for production of recombinant human proteins, including interleukin-1 β , -2, and -6 (8, 9). Especially, food-grade bacteria engineered to produce immunomodulatory molecules offer exciting potential to reduce chronic diseases. For example, the cheese starter lactic acid bacterium *Lactococcus lactis* MG1363 was engineered to secrete IL-10. In a mouse model of colitis, oral administration of recombinant *L. lactis* reduced intestinal inflammation, and the results of phase I clinical trial demonstrated safety (10). This seminal work laid the foundation to develop lactic acid bacteria as *in situ* TPP delivery vectors. The organism pertinent to this study, *Lactobacillus reuteri*, has proven to be functional as a therapeutic delivery platform in animal disease models (11). Advantages of using *L. reuteri* are the availability of high-throughput genome editing tools (12, 13) and its ability to thrive in the gut ecosystem, and *L. reuteri* has—compared to other lactobacilli and *L. lactis*—an extraordinarily low mutation rate (14), which is expected to improve the genetic stability of the recombinant organism. Lastly, *L. reuteri* ATCC PTA 6475, the strain we used in this study, has probiotic features, including amelioration of obesity (15) (Fig. 1a).

The goal of this study was to investigate to what extent engineered *L. reuteri* can further boost the native ability to ameliorate markers of diet-induced obesity. We demonstrated that the recombinant IL-22 delivered by *L. reuteri* is biologically active and that—compared to that of wild-type *L. reuteri*—the therapeutic efficacy was enhanced, specifically in the reduction of liver weight and triglycerides. This work, therefore, laid the foundation to develop *L. reuteri* as a next-generation probiotic to combat fatty liver disease.

RESULTS

Construction of a recombinant *L. reuteri* strain that secretes murine IL-22. We cloned a fusion of a *Lactobacillus reuteri* signal peptide and the coding sequence of murine interleukin-22 (mIL-22) in the high-copy number plasmid pJP028 (Table S1), which was established in *L. reuteri* to yield *L. reuteri* expressing IL-22. By ELISA, we demonstrated that *L. reuteri* expressing IL-22 produced up to 171 ng/ml of mIL-22 in LDM3 medium (Fig. 1b). We did not use MRS medium, as this interfered with enzyme-linked immunosorbent assay (ELISA) (data not shown). Also, Western blot analysis of a C-terminally FLAG-tagged version of mIL-22 without signal peptide revealed that mIL-22 migrates as a tetramer (Fig. 1b), which is in line with an observation made

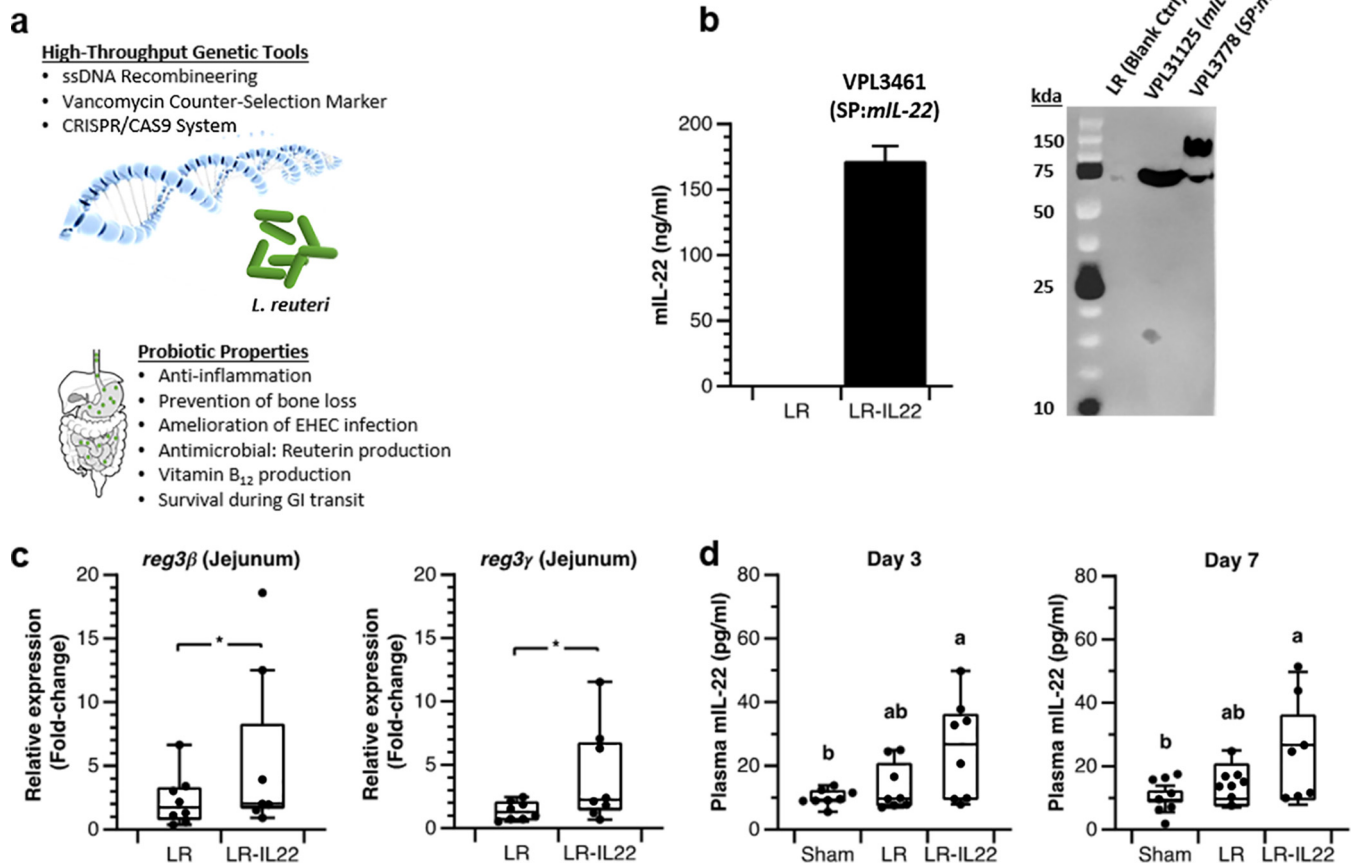


FIG 1 Probiotic properties of *L. reuteri* 6475 and systemic increase of biologically active mIL-22 by engineered *L. reuteri*. (a) Genetic tool availability (top) and beneficial probiotic properties (bottom). (b) (Left) mIL-22 ELISA on bacterial supernatant of wild-type *L. reuteri* and *L. reuteri* VPL3461 expressing mIL-22; (right) Western blot analysis of trichloroacetic acid (TCA)-precipitated proteins derived from *L. reuteri* supernatant (control [Ctrl]) and total lysates of *L. reuteri* strains VPL31125 and VPL3778 for mIL-22 production in LDM3 at 37°C and an OD₆₀₀ of 3.5. SP, signal peptide. (c and d) Eight-week-old male C57BL/6 mice ($n = 8$ per group) were administered nothing (sham), *L. reuteri* (10^9 cells/mouse), and *L. reuteri* expressing IL-22 (10^9 cells/mouse). (c) Fold change in *reg3β* (left) and *reg3γ* (right) gene expression in the jejunum after the consecutive oral administration of *L. reuteri* and *L. reuteri* expressing IL-22 for 7 days. Numbers indicate fold change relative to the mean value of the sham group. (d) Mice were gavaged daily for 7 days. Plasma mIL-22 levels were determined by ELISA. One-way ANOVA with Tukey's HSD test was used to determine the levels within three groups (a, b, or ab). The data in panels b to d represent averages of three biological replicates. For the box plots (c and d), center lines show the medians; box limits indicate the 25th and 75th percentiles. Error bars represent standard deviations. ns, no statistical significance. *, $P < 0.05$; **, $P < 0.01$ (t test).

previously (16). When we analyzed the supernatant of recombinant *L. reuteri* that is predicted to secrete mIL-22, we observed that only 18.3% of the recombinant protein was cleaved and migrated as a tetramer, whereas 81.7% recombinant protein appeared to be a fusion of the signal peptide and mIL-22, suggesting suboptimal processing of the signal peptide (Fig. 1b). The total amount of recombinant protein detected in the supernatant represented mature and unprocessed mIL-22 (data not shown).

***L. reuteri* produces biologically active mIL-22.** Since part of the recombinant protein appears to be dissociated from its signal sequence, i.e., mature, we tested next if mIL-22 delivered by *L. reuteri* was biologically active in the mouse intestinal tract. For 7 consecutive days, mice were gavaged daily with 10^9 cells of *L. reuteri* or *L. reuteri* expressing IL-22. Jejunum samples were harvested, followed by transcriptional analyses of *reg3β* and *reg3γ*, genes that are both regulated by IL-22 (4). Relative to the mice administered *L. reuteri* (LR group mice), mice administered *L. reuteri* expressing IL-22 (LR-IL-22 group mice) showed increased gene expression of *reg3β* (2.6-fold [$P = 0.03$]) and *reg3γ* (2.9-fold [$P = 0.04$]) (Fig. 1c). In the same mouse experiment, 1 week of

treatment with *L. reuteri* expressing IL-22 yielded a subtle but statistically significant increase in plasma mIL-22 levels compared to those in the sham group, but there was no difference from the LR group (Fig. 1d). While this is an interesting observation, at this point, it remains unclear what the underlying mechanism of the systemic increase of IL-22 following oral administration of *L. reuteri* VPL3461 is, and this warrants further investigation.

Recombinant *L. reuteri* reduces fatty liver in a mouse model of diet-induced obesity. Previously, we demonstrated that recombinant *L. reuteri*—which released mIL-22 following bacteriophage-mediated lysis—ameliorates steatohepatitis in a mouse model of alcohol-induced liver disease (11). To determine to what extent *L. reuteri*, and its recombinant derivative secreting mIL-22, impacts markers of metabolic syndrome, including fatty liver, we used a mouse model of diet-induced obesity. For 16 weeks, animals received a high-fat, high-sucrose diet (45% fat and 41% carbohydrate kcal). Starting at week 8 until the end of the trial (week 16), animals were subjected to daily treatment with LDM3 medium only (sham), *L. reuteri*, or *L. reuteri* expressing IL-22 (Fig. 2a). Following 7 weeks of treatment with *L. reuteri* expressing IL-22, mIL-22 plasma levels were significantly raised compared to those in the LR and the untreated control groups (Fig. 2b). However, before treatment (T0) with bacteria, the group to receive *L. reuteri* expressing IL-22 had elevated mIL-22 levels compared to those of the other treatment groups, yet differences were not statistically significant ($P > 0.05$). When we tracked the differences in plasma mIL-22 in each mouse over the 7-week period (T7 to T0), values were not found to be statistically different. Thus, while the data trended toward increased plasma mIL-22 levels following treatment with *L. reuteri* expressing IL-22, these data need to be interpreted with care given the increased basal levels of plasma mIL-22 in the LR-IL-22 group prior to the start of the treatment.

In terms of body weight gain and body fat composition, mice treated with *L. reuteri* or *L. reuteri* expressing IL-22 gained less weight (−47.7% LR versus sham [$P = 0.04$] and −39.2% LR-IL-22 versus sham [$P = 0.03$]) and had a lower body fat composition (−21.3% LR [$P = 0.004$] and −19.0% LR-IL-22 [$P = 0.003$]) and percent fat pad weight (−20.6% LR [$P = 0.01$] and −15.6% LR-IL-22 [$P = 0.03$]) than mice in the sham treatment group. The reduction in percent fat pad weight was representative of percent body fat, as determined by the body composition (percent fat mass) using nuclear magnetic resonance (NMR) (−7.8% LR [$P = 0.02$] and −6.4% LR-IL-22 [$P = 0.04$]). However, no statistical differences were observed when comparing these markers between the LR and LR-IL-22 groups (Fig. 2c and d).

The largest impact of treatment with recombinant probiotic was found in markers related to liver disease. The LR-IL-22 group displayed reduced percent liver weight compared to those of the LR group (−22.3% [$P = 0.002$]) and the sham group (−20.7% [$P < 0.001$]), while percent liver weight between the LR and the sham groups was not different ($P > 0.05$) (Fig. 2e). Liver triglyceride levels were also reduced in animals in the LR-IL-22 group compared to those in the LR treatment group (−4.6-fold [$P < 0.001$]) and the sham group (−11.4-fold [$P < 0.001$]). We determined that *L. reuteri* treatment also reduced liver triglyceride levels compared to those in the sham group (−2.5-fold [$P < 0.001$]) (Fig. 2f). Conclusively, in a model of diet-induced metabolic syndrome, wild-type *L. reuteri* inhibited weight gain and body fat accumulation and reduced liver fat and liver triglycerides; liver fat and triglycerides were further reduced following the delivery of *L. reuteri* expressing IL-22. Thus, these data emphasize the potential to explore a recombinant probiotic to combat nonalcoholic fatty liver disease, the most prevalent chronic liver disease worldwide (17).

DISCUSSION

In this study, we demonstrated the proof of concept that engineered *L. reuteri* can secrete biologically active mIL-22, which reduced markers related to liver disease in a model of diet-induced obesity. We believe that our study, combined with recent studies demonstrating the efficacy of recombinant *L. reuteri* in animal disease models of total

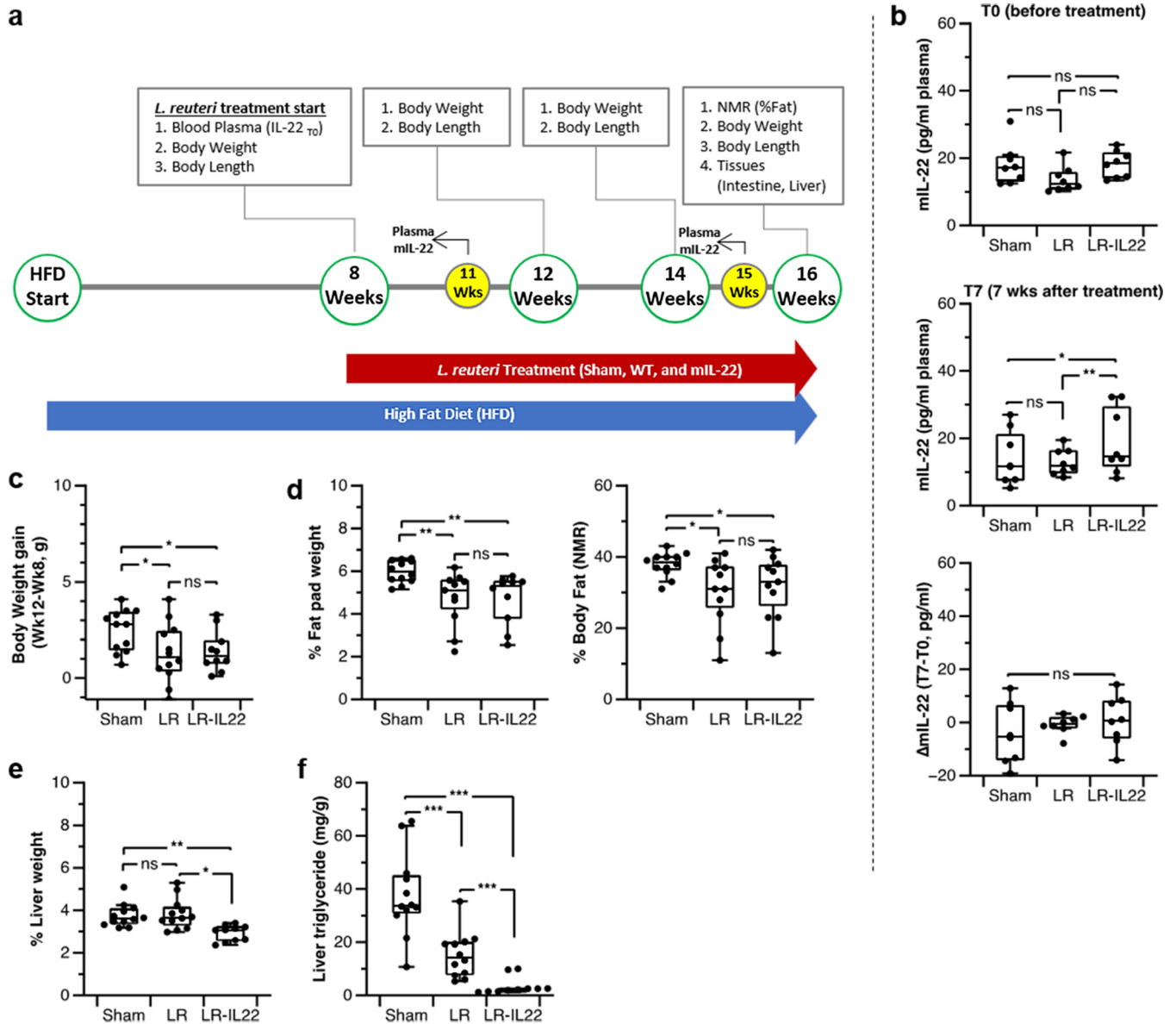


FIG 2 *L. reuteri* VPL3461 (LR-IL-22 group) improves diet-induced fatty liver disease. (a) Outline of high-fat-diet-induced obesity (DIO) *in vivo* model. Twelve mice per group were used for the sham, LR (wild-type), and LR-IL-22 (mIL-22) groups. Mice in the LR and LR-IL-22 groups were orally administered 10^9 CFU/mouse/day. (b) Plasma mIL-22 quantification. Blood plasma was isolated from the mice before and after the oral treatment. Plasma mIL-22 levels were determined by ELISA. (c) Mouse body weight monitored during treatment. Weight gain represents body weight difference between weeks 12 and 8 (T0). (d) Abdominal percent fat pad and total percent body fat at 16 weeks. (e) Percent liver weight. Whole liver weights were compared for the three groups at 16 weeks. For panels d and e, fat compositions and liver weight were calculated per body weight. (f) One-hundred-milligram left top liver lobe samples were collected from the whole liver, followed by quantification of liver triglyceride. For panels b to f, center lines show the medians; box limits indicate the 25th and 75th percentiles. Error bars represent standard deviation. *, $P < 0.05$; **, $P < 0.01$; ***, $P < 0.001$ (*t* test).

body irradiation and alcohol-induced liver disease (11, 18), reveals the potential to develop *L. reuteri* as a next-generation probiotic to treat disease in the clinic.

To export recombinant mIL-22, we relied on the native bacterial secretion machinery. As is evident from our Western blot analysis, only part of the recombinant protein was processed correctly by the bacterial cell secretion machinery. We made a similar observation with leptin (14). While incomplete cleavage may be overcome by testing different leader sequences or by optimizing the combination of the leader sequence and the N-terminal sequence of the mature protein, these are not trivial tasks (19). Alternative approaches may therefore be more efficient. For example, we recently demonstrated that activation of native prophages in *L. reuteri* can lyse the cell and

subsequently release a recombinant mature protein that has accumulated inside the cell; this approach has proven successful in preclinical disease models (11, 18). Using bacterial lysis to release mature proteins also has the advantage that lysis can be optimized to contribute to containment. Future studies will investigate differences in the therapeutic efficacy between the two probiotic delivery systems in the diet-induced obesity model.

Regardless of the partial processing of mIL-22, we observed in mice fed a regular chow and administered *L. reuteri* expressing IL-22 a subtle but significant increase in systemic IL-22 levels (Fig. 1d), which was also observed in mice following 7 weeks of treatment with a high-fat diet (HFD) and *L. reuteri* expressing IL-22 (Fig. 2b). While future studies need to validate the biological relevance of differences in systemic IL-22 during HFD treatment, probiotic-driven delivery of mIL-22 clearly impacts host physiology. For example, after 8 weeks of treatment with an HFD combined with *L. reuteri* expressing IL-22, the total body length of mice—based on nose-tail measurements—was greater than that of animals that received *L. reuteri* or sham treatment (Fig. S1a), and our data show a weak correlation between body length and growth hormone level during treatment with *L. reuteri* expressing IL-22 (Fig. S1). El-Zayadi et al. recently showed that IL-22 has a postinflammation osteogenic property in the absence of gamma interferon (IFN- γ) and tumor necrosis factor (TNF) by regulating mesenchymal stem cells (MSC), which play a role in new bone formation and repair (20). The largest impact of probiotic-mediated delivery of IL-22 in our model of diet-induced obesity was reduction of liver triglycerides. Indeed, IL-22 has several metabolic benefits, as it decreases chronic inflammation and regulates lipid metabolism in liver and adipose tissues (4, 5). In mice, IL-22 elicits hepatoprotective properties via the activation of STAT3 (3, 5, 21); STAT3 downregulates the expression of lipogenic genes—and consequently reduces fat accumulation—and upregulates the expression of antiapoptotic genes, including *reg3*. Because the IL-22/STAT3/*reg3* axis exists in the intestine (21), it is plausible that IL-22 upregulates REG3 β and REG3 γ in jejunum via STAT3. Especially, REG3 is a multifunctional enzyme overexpressed by IL-22 induction and known to reduce injury in liver and intestine. Antiapoptotic activity of REG3 β and REG3 γ in liver and gut epithelium is essential in tissue regeneration via activation of protein kinase A, while antimicrobial activity of intestinal REG3 prevents translocation of bacteria to the liver (11, 21).

Treatment with *L. reuteri* expressing IL-22 yielded subtle but statistically significant changes in the expression of *reg3* genes in the small intestine and in IL-22 levels in the plasma. However, not all animals responded to treatment with *L. reuteri* expressing IL-22. At this point, the rationales for different responses among animals within the same treatment group are merely speculative. Perhaps differences in the microbiota between mice housed in different cages could affect *L. reuteri* physiology and IL-22 production. Also, additional insight in the production of IL-22 throughout the gastrointestinal tract, along with measuring *reg* expression and plasma IL-22 levels in diseased mice, will be helpful to better understand the observed inconsistencies between animals. For future studies—if direct comparisons were to be made between different animal trials—it is expected that animals representing the control groups would be treated identically, though this was not a concern in the current study. The use of REG3 mutant mice, as previously described in a model of ethanol-induced liver disease (11), could provide more mechanistic insight how recombinant IL-22 reduces fatty liver disease in our model. As of now, the lack of such studies represents a limitation of our work; nevertheless, our observations provide a clear foundation for the above-mentioned future studies to gain a deeper mechanistic understanding of how *L. reuteri*-mediated delivery of IL-22 ameliorates fatty liver disease. Finally, while recombinant (probiotic) bacteria hold the potential to treat and prevent disease, the development and assessment of environmental and biological containment systems are critically important to bring these engineered bacteria a step closer to the clinic.

MATERIALS AND METHODS

Bacterial strains, plasmids, and media. All bacterial strains and plasmids used in this study are listed in Table S1. *Lactobacillus reuteri* 6475 and its derivatives were cultured at 37°C in deMan Rogosa Sharpe (MRS) medium (Difco, BD Biosciences). Where appropriate, erythromycin was added to a final concentration of 5 µg/ml for *L. reuteri*. Electrocompetent cells of *L. reuteri* were prepared as described before (22). To test mL-22 expression and to prepare bacteria for animal experiments, *L. reuteri* was cultured in lactobacillus defined medium III (LDM3) (23).

Reagents and enzymes. Cloning was performed via ligase cycling reaction (LCR) (24). Enzymes and reagents for LCR were purchased from Lucigen. PCR for cloning purposes was performed with the high-fidelity enzyme Phusion Hot Start polymerase II (Fermentas). PCR for screening purposes was performed with *Taq* polymerase (Denville Scientific). To concentrate the LCR before electrotransformation into *L. reuteri*, we used Pellet Paint coprecipitant (Novagen). Oligonucleotides and synthetic double-stranded DNA fragments were purchased from Integrated DNA Technologies (IDT). All oligonucleotides and synthetic DNA fragments used in this study are listed in Table S2.

Plasmid construction for mL-22 secretion from *L. reuteri* 6475. We engineered *Lactobacillus reuteri* 6475 to secrete the murine cytokine interleukin-22 (mIL-22). We opted for expression from the multicopy plasmid pJP028 (a gift from Robert Britton) to maximize mL-22 production (Table S1). By PCR (oVPL1221 and oVPL1222) we amplified the backbone of pJP028, omitting the cell wall anchor domain, to yield a 4.579-kb product. For optimal expression of mL-22 in our expression host *L. reuteri*, we first applied *in silico* codon optimization of the mL-22 coding sequence using the online software OPTIMIZER (<http://genomes.urv.es/OPTIMIZER/>), followed by gBLOCK (IDT) synthesis. The synthetic product (gVPL1 [Table S2]) was amplified by PCR (oVPL1219 and oVPL1220), followed by fusion to the pJP028 backbone by LCR (24). The LCR mixture was precipitated and transformed *L. reuteri* 6475. Transformants were screened by PCR (oVPL329 and oVPL363) to confirm the cloning of mL-22. One positive clone was colony purified, a 1.584-kb mL-22 secretion cassette was confirmed by colony PCR, and the integrity of the construct was confirmed by DNA sequencing (GeneWiz). The resultant strain was named VPL3461.

To insert a C-terminal 3× FLAG tag in IL-22, we used oVPL2113 and oVPL2114, which contain 3× FLAG sequence tags, and performed inverse PCR of the plasmid backbone followed by self-circularization. The resultant plasmids were named pVPL3776 (SP:IL-22:3X FLAG) and pVPL31125 (IL-22:3X FLAG) (Table S1).

Culture conditions for mL-22 secretion. *L. reuteri* 6475 stored at –80°C was inoculated into 10 ml of MRS broth, and *L. reuteri* VPL3461 was inoculated into 10 ml of MRS medium containing 5 µg/ml of erythromycin at 37°C. An overnight culture of each strain was subcultured into the same medium (10 ml), and initial optical density at 600 nm (OD₆₀₀) was set at 0.1. Cells from each culture were harvested at mid-log phase (OD₆₀₀ = 1.0 to ~1.2) by centrifugation at 5,000 rpm for 5 min. Cells were washed twice in LDM3 containing glycerol (15%, vol/vol). Washed-cell pellet was kept at –80°C until use or resuspended in 10 ml of fresh prewarmed LDM3 and incubated at 37°C until reaching an OD₆₀₀ of 3.5 to ~3.7. Cells in LDM3 were 10-fold concentrated in 1 ml of LDM3 culture supernatant after centrifugation at 3,214 × *g* for 5 min. One hundred microliters of concentrated cell suspension in LDM3 was used for oral administration, and the supernatant was used to quantify mL-22 level by ELISA (R&D Systems).

mIL-22 analysis. *L. reuteri* strains 6475 and VPL3461 were cultured in LDM3 as described under “Culture conditions for mL-22 secretion,” and the supernatants were collected after centrifugation (5 min at 3,214 × *g*), followed by filter sterilization (0.22 µm; Millipore). One hundred microliters of filter-sterilized supernatant from *L. reuteri* 6475 and VPL3461 was assessed for the presence of mL-22 by ELISA (R&D Systems).

For Western blot analysis, samples from *L. reuteri* strains engineered to secrete or intracellularly accumulate mL-22 (VPL3778 or VPL31125, respectively) were prepared as previously described (14), with the exception that protein from VPL3778 was precipitated from a higher volume of culture (35 ml).

mIL-22 treatment in a mouse model. Twenty-four 6-week-old male B6 mice (C57BL/6J) were purchased from The Jackson Laboratory (Bar Harbor, ME). Animals were housed at an environmentally controlled facility with a 12-h light and dark cycle. Both diet (Formulab 5008; LabDiet, St. Louis, MO) and water were freely available to the animals. After transport, animals were allowed to adjust to the new environment for 2 weeks, after which treatment by oral gavage started. Three groups (*n* = 8 per group) were treated daily for 7 consecutive days. Treatments were a sham gavage in which the animals were subjected to insertion of a gavage needle without administering anything (sham group), *L. reuteri* 6475 (LR group), and *L. reuteri* VPL3461 (LR-IL-22 group). The bacterial load administered per mouse was ~1 × 10⁹ CFU in a volume of 100 µl of the respective bacterial supernatant.

A mouse model of high-fat-diet-induced metabolic syndrome. Thirty-two 6-week-old male C57BL/6J mice were purchased from The Jackson Laboratory (Bar Harbor, ME). The animals were housed (*n* = 3 per cage) in an environmentally controlled facility with a 12-h light and 12-h dark cycle for 8 weeks on a high-fat diet (TD.08811; Envigo) before *L. reuteri* treatment. Food and water were provided *ad libitum* during the mouse experiment. After 8 weeks on the high-fat diet, mice (*n* = 12 per group) were gavaged daily for 2 consecutive months with 100 µl of LDM3 (sham group), a culture containing 10⁹ CFU/ml of *L. reuteri* 6475 (LR group), or a culture containing 10⁹ CFU/ml of *L. reuteri* VPL3461 (LR-IL-22 group). Retro-orbital bleeding was performed at 8, 11, and 15 weeks. Body weight and length were monitored every other week. At the endpoint (16 weeks), body composition was monitored via NMR analysis followed by CO₂ euthanization for sampling tissues (Fig. 2a).

Blood plasma isolation. Two hours after the last gavage, 50 µl of blood per mouse was collected via retro-orbital puncture using heparin-coated capillary tubes (Fisher Scientific). Plasma was isolated

from the whole-blood sample by centrifugation at 9,000 rpm for 7 min, and the plasma fraction was stored at -80°C until use. By ELISA (as described above), we determined plasma mL-22 levels.

NMR body composition analysis. After the 16 weeks on the HFD, total body fat composition from the live animals was measured by using NMR (4-in-1-1000 analyzer; EchoMRI, Houston, TX). Percent fat composition was calculated based on the amount of body fat on total mass (fat plus lean).

Liver triglyceride analysis. Liver triglycerides (TGs) were quantified following the Jouihan method (25). One hundred milligrams of frozen liver tissue was homogenized, and total lipids were extracted in ethanolic KOH at 55°C for 16 h. Triglyceride content was determined by colorimetric analysis using free glycerol reagent (Sigma-Aldrich; F6428) and glycerol standard (Sigma-Aldrich; G7793).

cDNA synthesis. To assess the biological functionality of *L. reuteri*-secreted mL-22, we assessed gene expression levels of *reg3 β* and *reg3 γ* . Part of the small intestine (jejunum) of each animal was processed for RNA isolation. First, samples were homogenized (Omni TH; Omni International), followed by RNA isolation and on-column DNase I treatment (Qiagen). Following isolation, additional DNase I treatment was conducted (RQ1 DNase; Promega), followed by quantification using a Qubit fluorometer (Invitrogen). One microgram of RNA was reverse transcribed using an iScript cDNA synthesis kit (Bio-Rad Laboratories).

Quantitative real-time PCR. Relative gene expression levels were determined using CFX96 real-time PCR (RT-PCR; Bio-Rad). Expression of *reg3 β* and *reg3 γ* was determined relative to that of the housekeeping gene *β -actin*. The quantitative RT-PCR (qRT-PCR) was performed with SYBR green PCR master mix (Bio-Rad). Primers for amplification of *reg3 β* (oVPL1313 and oVPL1314), *reg3 γ* (oVPL1315 and oVPL1316), and *β -actin* (oVPL1325 and oVPL1326) are listed in Table S2. Relative gene expression of the *reg3* gene in the jejunum tissues compared to *β -actin* was determined by the Relative Expression Software Tool (REST), which allows comparison of gene expression between groups of animals (26).

Statistical analysis. Analysis of variance (ANOVA) was used for data analysis, with Tukey's honestly significant difference (HSD) *post hoc* comparison to investigate differences in body weight, percent fat pad and liver weight, liver triglyceride, and plasma IL-22. Significance in comparisons between groups was analyzed by *t* test. A significant difference was considered when the *P* value was lower than 0.05.

SUPPLEMENTAL MATERIAL

Supplemental material is available online only.

FIG S1, TIF file, 0.1 MB.

TABLE S1, DOCX file, 0.01 MB.

TABLE S2, DOCX file, 0.01 MB.

ACKNOWLEDGMENTS

The Van Pijkeren Laboratory is grateful for funding received from the University of Wisconsin—Madison Food Research Institute (233PRJ75PW), the UW-Madison Graduate School (135 AAA2218), and the UW-Madison Institute of Clinical and Translational Research, funded by National Center for Advancing Translational Science award UL1TR000427. This work was also supported by the U.S. Department of Agriculture, National Institute of Food and Agriculture (USDA NIFA) Hatch award MSN185615, and grant no. 2018-6717-27523.

We thank David Nelson for his guidance on using NMR.

J.-H.O. designed and performed experiments, analyzed and interpreted data, and wrote the manuscript. K.L.S., D.S.S., and L.M.A. helped perform experiments. C.-L.E.Y., M.A.K., and A.D.A. provided instruments, research space, and technical support, and J.P.V.P. secured funding, conceived, designed, and supervised the study, and critically revised the manuscript.

J.P.V.P. received unrestricted funds from BioGaia AB (Stockholm, Sweden).

REFERENCES

1. Grundy SM, Brewer HB, Jr, Cleeman JI, Smith SC, Jr, Lenfant C, National Heart, Lung, and Blood Institute. 2004. Definition of metabolic syndrome: report of the National Heart, Lung, and Blood Institute/American Heart Association conference on scientific issues related to definition. *Circulation* 109:433–438. <https://doi.org/10.1161/01.CIR.0000111245.75752.C6>.
2. Armstrong C. 2006. AHA and NHLBI review diagnosis and management of the metabolic syndrome. *Am Fam Physician* 74:1039–1047.
3. Caparrós E, Francés R. 2018. The interleukin-20 cytokine family in liver disease. *Front Immunol* 9:1155. <https://doi.org/10.3389/fimmu.2018.01155>.
4. Wang X, Ota N, Manzanillo P, Kates L, Zavala-Solorio J, Eidenschek C, Zhang J, Lesch J, Lee WP, Ross J, Diehl L, van Bruggen N, Kolumam G, Ouyang W. 2014. Interleukin-22 alleviates metabolic disorders and restores mucosal immunity in diabetes. *Nature* 514:237–241. <https://doi.org/10.1038/nature13564>.
5. Pan C-X, Tang J, Wang X-Y, Wu F-R, Ge J-F, Chen F-H. 2014. Role of interleukin-22 in liver diseases. *Inflamm Res* 63:519–525. <https://doi.org/10.1007/s00011-014-0727-3>.
6. Cyriac JM, James E. 2014. Switch over from intravenous to oral therapy: a concise overview. *J Pharmacol Pharmacother* 5:83–87. <https://doi.org/10.4103/0976-500X.130042>.
7. Muheem A, Shakeel F, Jahangir MA, Anwar M, Mallick N, Jain GK, Warsi MH, Ahmad FJ. 2016. A review on the strategies for oral delivery of proteins and peptides and their clinical perspectives. *Saudi Pharm J* 24:413–428. <https://doi.org/10.1016/j.jsps.2014.06.004>.
8. Carrier M, Chatfield S, Dougan G, Nowicka U, O'Callaghan D, Beesley J, Milano S, Cillari E, Liew F. 1992. Expression of human IL-1 beta in

- Salmonella typhimurium. A model system for the delivery of recombinant therapeutic proteins in vivo. *J Immunol* 148:1176–1181.
9. Steidler L, Robinson K, Chamberlain L, Schofield KM, Remaut E, Le Page RW, Wells JM. 1998. Mucosal delivery of murine interleukin-2 (IL-2) and IL-6 by recombinant strains of *Lactococcus lactis* coexpressing antigen and cytokine. *Infect Immun* 66:3183–3189. <https://doi.org/10.1128/IAI.66.7.3183-3189.1998>.
 10. Braat H, Rottiers P, Hommes DW, Huyghebaert N, Remaut E, Remon JP, Van Deventer SJ, Neiryck S, Peppelenbosch MP, Steidler L. 2006. A phase I trial with transgenic bacteria expressing interleukin-10 in Crohn's disease. *Clin Gastroenterol Hepatol* 4:754–759. <https://doi.org/10.1016/j.cgh.2006.03.028>.
 11. Hendriks T, Duan Y, Wang Y, Oh J-H, Alexander LM, Huang W, Stärkel P, Ho SB, Gao B, Fiehn O, Emond P, Sokol H, van Pijkeren J-P, Schnabl B. 2019. Bacteria engineered to produce IL-22 in intestine induce expression of REG3G to reduce ethanol-induced liver disease in mice. *Gut* 68:1504–1515. <https://doi.org/10.1136/gutjnl-2018-317232>.
 12. Oh J-H, van Pijkeren J-P. 2014. CRISPR–Cas9-assisted recombineering in *Lactobacillus reuteri*. *Nucleic Acids Res* 42:e131. <https://doi.org/10.1093/nar/gku623>.
 13. Zhang S, Oh J-H, Alexander LM, Özçam M, Van Pijkeren J-P. 2018. D-Alanyl-D-alanine ligase as a broad-host-range counterselection marker in vancomycin-resistant lactic acid bacteria. *J Bacteriol* 200:e00607-17. <https://doi.org/10.1128/JB.00607-17>.
 14. Alexander LM, Oh J-H, Stapleton DS, Schueler KL, Keller MP, Attie AD, van Pijkeren J-P. 2019. Exploiting prophage-mediated lysis for biotherapeutic release by *Lactobacillus reuteri*. *Appl Environ Microbiol* 85:e02335-18. <https://doi.org/10.1128/AEM.02335-18>.
 15. Britton R. 2017. *Lactobacillus reuteri*, p 89–97. In Floch MH, Ringel Y, Walker WA (ed), *The microbiota in gastrointestinal pathophysiology: implications for human health, prebiotics, probiotics and dysbiosis*. Elsevier, London, United Kingdom.
 16. de Oliveira Neto M, Ferreira JR, Jr, Colau D, Fischer H, Nascimento AS, Craievich AF, Dumoutier L, Renauld J-C, Polikarpov I. 2008. Interleukin-22 forms dimers that are recognized by two interleukin-22R1 receptor chains. *Biophys J* 94:1754–1765. <https://doi.org/10.1529/biophysj.107.112664>.
 17. Li J, Zou B, Yeo YH, Feng Y, Xie X, Lee DH, Fujii H, Wu Y, Kam LY, Ji F, Li X, Chien N, Wei M, Ogawa E, Zhao C, Wu X, Stave CD, Henry L, Barnett S, Takahashi H, Furusyo N, Eguchi Y, Hsu Y-C, Lee T-Y, Ren W, Qin C, Jun DW, Toyoda H, Wong V-S, Cheung R, Zhu Q, Nguyen MH. 2019. Prevalence, incidence, and outcome of non-alcoholic fatty liver disease in Asia, 1999–2019: a systematic review and meta-analysis. *Lancet Gastroenterol Hepatol* 4:389–398. [https://doi.org/10.1016/S2468-1253\(19\)30039-1](https://doi.org/10.1016/S2468-1253(19)30039-1).
 18. Zhang X, Fisher R, Hou W, Shields D, Epperly MW, Wang H, Wei L, Leibowitz BJ, Yu J, Alexander LM, van Pijkeren J-P, Watkins S, Wipf P, Greenberger JS. 2020. Second-generation probiotics producing IL-22 increase survival of mice after total body irradiation. *In Vivo* 34:39–50. <https://doi.org/10.21873/invivo.11743>.
 19. Peng C, Shi C, Cao X, Li Y, Liu F, Lu F. 2019. Factors influencing recombinant protein secretion efficiency in Gram-positive bacteria: signal peptide and beyond. *Front Bioeng Biotechnol* 7:139. <https://doi.org/10.3389/fbioe.2019.00139>.
 20. El-Zayadi AA, Jones EA, Churchman SM, Baboolal TG, Cuthbert RJ, El-Jawhari JJ, Badawy AM, Alase AA, El-Sherbiny YM, McGonagle D. 2016. Interleukin-22 drives the proliferation, migration and osteogenic differentiation of mesenchymal stem cells: a novel cytokine that could contribute to new bone formation in spondyloarthropathies. *Rheumatology* 56:488–493.
 21. Chen Z, Downing S, Tzanakakis ES. 2019. Four decades after the discovery of regenerating islet-derived (Reg) proteins: current understanding and challenges. *Front Cell Dev Biol* 7:235. <https://doi.org/10.3389/fcell.2019.00235>.
 22. Ahrné S, Molin G, Axelsson L. 1992. Transformation of *Lactobacillus reuteri* with electroporation: studies on the erythromycin resistance plasmid pLUL631. *Curr Microbiol* 24:199–205.
 23. Thomas CM, Hong T, van Pijkeren JP, Hemarajata P, Trinh DV, Hu W, Britton RA, Kalkum M, Versalovic J. 2012. Histamine derived from probiotic *Lactobacillus reuteri* suppresses TNF via modulation of PKA and ERK signaling. *PLoS One* 7:e31951. <https://doi.org/10.1371/journal.pone.0031951>.
 24. de Kok S, Stanton LH, Slaby T, Durot M, Holmes VF, Patel KG, Platt D, Shapland EB, Serber Z, Dean J, Newman JD, Chandran SS. 2014. Rapid and reliable DNA assembly via ligase cycling reaction. *ACS Synth Biol* 3:97–106. <https://doi.org/10.1021/sb4001992>.
 25. Jouihan H. 2012. Measurement of liver triglyceride content. *Bio Protoc* 2:e223. <https://doi.org/10.21769/BioProtoc.223>.
 26. Pfaffl MW, Horgan GW, Dempfle L. 2002. Relative expression software tool (REST®) for group-wise comparison and statistical analysis of relative expression results in real-time PCR. *Nucleic Acids Res* 30:e36. <https://doi.org/10.1093/nar/30.9.e36>.